Rab11 regulates exocytosis of recycling vesicles at the plasma membrane

Senye Takahashi[1], Keiji Kubo[1], Satoshi Waguri[2], Atsuko Yabashi[2], Hye-Won Shin[1,3], Yohei Katoh[1] and Kazuhisa Nakayama[1,*]

[1]Graduate School of Pharmaceutical Sciences, Kyoto University, Sakyo-ku, Kyoto 606-8501, Japan
[2]Department of Anatomy and Histology, Fukushima Medical University School of Medicine, Fukushima City, Fukushima 960-1295, Japan
[3]Career-path Promotion Unit for Young Life Scientists, Kyoto University, Sakyo-ku, Kyoto 606-8501, Japan
*Author for correspondence (kazunaka@pharm.kyoto-u.ac.jp)

Accepted 9 May 2012
Journal of Cell Science 125, 4049–4057

doi: 10.1242/jcs.102913

Summary

Rab11 is known to associate primarily with perinuclear recycling endosomes and regulate recycling of endocytosed proteins. However, the recycling step in which Rab11 participates remains unknown. We show here that, in addition to causing tubulation of recycling endosomes, Rab11 depletion gives rise to accumulation of recycling carriers containing endocytosed transferrin and transferrin receptor beneath the plasma membrane. We also show that the carriers are transported from perinuclear recycling endosomes to the cell periphery along microtubules. Total internal reflection fluorescence microscopy of cells expressing EGFP-tagged transferrin receptor revealed that Rab11 depletion inhibits tethering and fusion of recycling carriers to the plasma membrane. Depletion of Sec15, which interacts with Rab11, or Exo70, both components of the exocyst tethering complex, leads to essentially the same phenotypes as those of Rab11 depletion. Thus, in addition to its role in recycling processes at perinuclear recycling endosomes, Rab11 is transported along microtubules to the cell periphery through association with recycling carriers, and directly regulates vesicle exocytosis at the plasma membrane in concert with the exocyst.

Key words: Rab11, Recycling endosome, Transferrin receptor, Exocyst

Introduction

Cells internalize extracellular materials, plasma membrane (PM) proteins and their ligands by endocytosis. Some of endocytosed proteins recycle back to the cell surface for reuse, whereas others are destined for degradation in lysosomes. The most extensively investigated recycling protein is transferrin receptor (TfnR) (Grant and Donaldson, 2009; Maxfield and McGraw, 2004; Mukherjee et al., 1997). It binds diferric transferrin (Tfn) on the cell surface, and is internalized via clathrin-coated vesicles and delivered to early/sorting endosomes. Subsequently, the Tfn–TfnR complex is returned to the PM either directly (rapid recycling) or indirectly via recycling endosomes (REs) (slow recycling). REs, whose subcellular localization varies among cell types, are often located near the nucleus or centrosome and consequently referred to as perinuclear or pericentrosomal REs (Grant and Donaldson, 2009; Mukherjee et al., 1997).

Rab family small GTPases regulate various aspects of membrane traffic through interactions with their effector proteins (Schwartz et al., 2007; Stenmark, 2009). Among them, Rab11 is one of extensively studied Rab GTPases. Rab11 associates primarily with REs and regulates recycling of endocytosed proteins; it has therefore been used as an RE marker in a number of studies (Grant and Donaldson, 2009; Stenmark, 2009; van Ijzendoorn, 2006). However, the recycling step that Rab11 regulates remains poorly understood: For example, previous studies showed that expression of a dominant-negative Rab11a mutant, Rab11a(S25N), inhibited release of endocytosed ^{125}I-labelled Tfn to the extracellular medium (Ren et al., 1998; Ullrich et al., 1996) and induced tubulation of compartments containing endocytosed Tfn and TfnR (Hölttä-Vuori et al., 2002; Wilcke et al., 2000). However, the relationship between inhibition of Tfn recycling and tubulation of TfnR-containing compartments has remained unclear; In previous studies with *Drosophila* cells, mutation or inhibition of Rab11 and the exocyst tethering complex was reported to cause intracellular accumulation of DE-cadherin and Delta, yet it was not determined where these proteins were accumulated (Guichard et al., 2010; Langevin et al., 2005). On the other hand, Rab11 was reported to transiently associate with fusion sites of Fc receptor–containing vesicles with the PM, but it is not yet known whether the Rab11 association with fusion sites is critical for the fusion event (Ward et al., 2005).

Over the course of our experiments, we noticed that, in addition to their distribution in the perinuclear region, endogenous Rab11 and TfnR are found in the peripheral region, particularly around the cellular tips, albeit at a relatively low frequency. In this study, we extend this finding to show that Rab11 not only associates with perinuclear REs, but also participates in exocytosis of recycling vesicles at the PM in concert with the exocyst tethering complex.

Results

Peripheral localization of Rab11 and TfnR

In HeLa cells, vesicular RE structures visualized by immunostaining for Rab11 and TfnR are found throughout the cytoplasm, relatively concentrated in the perinuclear region.

However, we noticed that Rab11 and TfnR are also found in the peripheral region, particularly around the cellular tips (Fig. 1A). By time-lapse analysis of cells expressing EGFP-tagged Rab11a, we observed vesicular structures throughout the cytoplasm, relatively concentrated in the tip regions, and often moving in an intermittent manner that is suggestive of microtubule-based transport (Fig. 1B; supplementary material Movie 1). When the EGFP–Rab11a signals around the cellular tips were photobleached, the signals were gradually recovered and centrifugal movement of EGFP–Rab11a-positive vesicular structures was often observed in the photobleached area (Fig. 1C; supplementary material Movie 2), suggesting that the peripheral Rab11-positive intermediates are delivered, at least in part, from perinuclear REs.

We next compared localization of Rab11 against organelle marker proteins (supplementary material Fig. S1). Neither EEA1 (early endosomes), Lamp-1 (late endosomes/lysosomes) nor GM130 (Golgi) was significantly colocalized with Rab11. In contrast, EGFP-tagged DMT1-II (type II isoform of divalent metal transporter 1) was extensively colocalized with Rab11 in the tip regions; DMT1-II is localized primarily to REs, and is responsible for transport across endosomal membranes of iron internalized via the Tfn–TfnR complex (Lam-Yuk-Tseung and Gros, 2006; Tabuchi et al., 2002). Taken together, these observations indicate that peripheral Rab11-positive structures represent REs or carrier intermediates originating from REs.

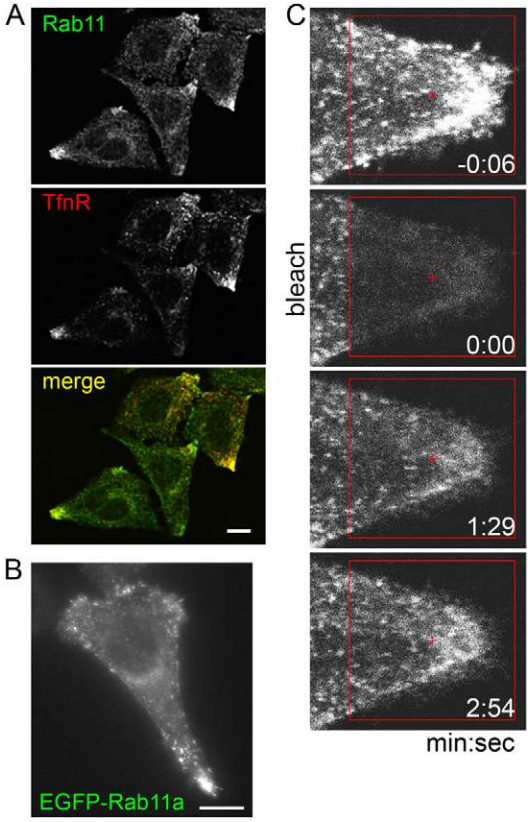

Fig. 1. Peripheral localization of Rab11 and TfnR. (**A**) HeLa cells were doubly immunostained for Rab11 and TfnR. A representative image of cells clearly exhibiting peripheral localization of Rab11 and TfnR is shown. (**B**) HeLa cells were transfected with an expression vector encoding N-terminally EGFP-tagged Rab11a, and subjected to time-lapse recording. A representative frame from supplementary material Movie 1 is shown. Scale bars: 10 μm. (**C**) FRAP analysis of cells expressing EGFP–Rab11. HeLa cells expressing EGFP–Rab11a were subjected to FRAP analysis. At time=0, the boxed area was photobleached and signal recovery was followed by time-lapse recording. Representative frames from supplementary material Movie 2 are shown.

Rab11 depletion gives rise to peripheral accumulation of recycling carriers as well as tubulation of perinuclear REs

We then set out to investigate the effects of Rab11 depletion on perinuclear and peripheral localization of TfnR. In mammals there are two Rab11 isoforms, both of which are expressed in HeLa cells (Fig. 2A). Using a previously characterized double-stranded siRNA (Junutula et al., 2004; Takahashi et al., 2011), we could almost completely deplete Rab11a in HeLa cells (Fig. 2B, top panel). Because of a lack of Rab11b-specific antibody, we were unable to directly measure depletion of Rab11b; however, we believe that Rab11b is also specifically depleted, on the basis of data obtained using siRNAs for Rab11a and Rab11b in combination with Rab11a-specific antibody (top panel) and an antibody that recognizes both Rab11 isoforms (middle panel).

When morphologically examined, Rab11b knockdown did not alter TfnR-positive structures (Fig. 2C, compare column 3 with column 1; Fig. 2D), whereas Rab11a depletion had a subtle, but significant, effect (Fig. 2C, column 2; Fig. 2D); TfnR was often found on tubules emanating from perinuclear structures and tended to accumulate around the cellular tips. Depletion of both Rab11 isoforms had the most dramatic impact (Fig. 2C, column 4; Fig. 2D); the double knockdown reduced the number of perinuclear vesicular structures positive for TfnR while inducing tubules reminiscent of those observed in cells expressing dominant-negative Rab11a (Hölttä-Vuori et al., 2002; Wilcke et al., 2000) (see below). Furthermore, simultaneous depletion of both Rab11 isoforms enhanced TfnR accumulation in the tip regions.

We next evaluated the impact of Rab11 depletion on trafficking through REs. To this end, we treated HeLa cells with Alexa-Fluor-555-conjugated Tfn at 4℃ to allow binding to surface TfnR; after washing out excess fluorescent Tfn, we incubated the cells at 37℃ to follow Tfn trafficking. In control cells, after 2.5–10 min incubation at 37℃, fluorescent Tfn was found on punctate structures positive for EEA1 (supplementary material Fig. S2A) and TfnR (Fig. 3A) that represent early and recycling endosomes. After 20 min, however, fluorescent Tfn became barely detectable within the cells, indicating release of Tfn molecules to the extracellular medium. In cells depleted of both Rab11 isoforms (Fig. 3B), fluorescent Tfn and TfnR were predominantly found around the tips after 10–30 min at 37℃. After 60 min, however, fluorescent Tfn disappeared almost completely from the cells, indicating that Rab11 knockdown delays, but does not completely block, Tfn release. A significant fraction of fluorescent Tfn reached EEA1-positive punctate structures after 5–10 min incubation at 37℃, indicating that endocytosis of Tfn can occur under the Rab11-depleted conditions (supplementary material Fig. S2B). Moreover, after 10–20 min incubation, Tfn was accumulated at the cell tips where EEA1 was not found. It suggests that the internalized Tfn have left EEA1-positive early endosomes after 10–20 min incubation and thus the accumulation of Tfn at the cell tips are due to the exocytic but not to endocytic defect. Similarly to Rab11 knockdown, expression of dominant-negative Rab11a,

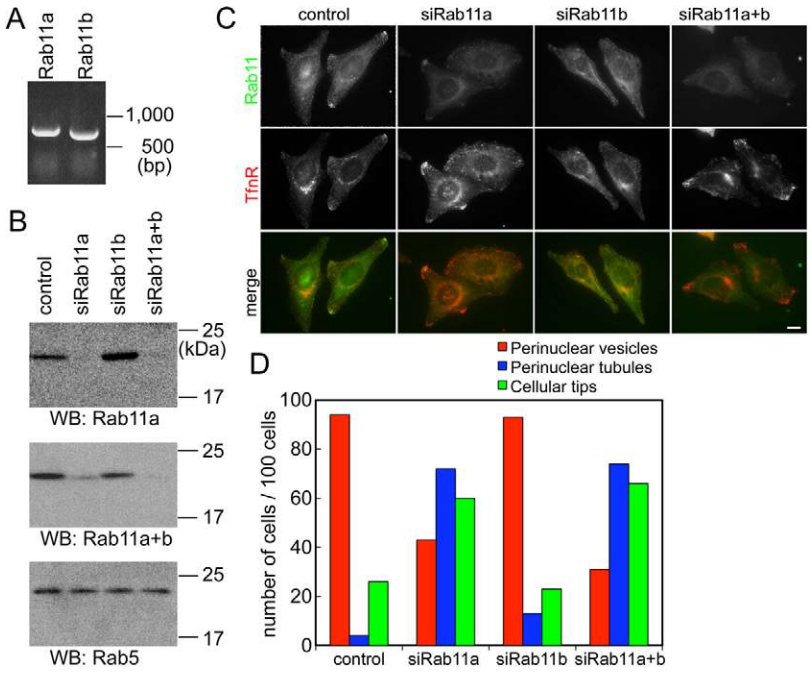

Fig. 2. Endogenous expression and knockdown of Rab11a and Rab11b in HeLa cells. (**A**) RT-PCR analysis for expression of Rab11a and Rab11b mRNAs. Total RNAs from HeLa cells were subjected to RT-PCR using the following primer sets: Rab11a, forward, 5′-CCCACAGATACCACTGCTGC-3′, and reverse, 5′-CGGAATTCTTAGATGTTCTGACAGCACTGC-3′; Rab11b, forward, 5′-GAAGCGCCAGGACAATGGGG-3′, and reverse, 5′-CGCTCGAGTCACAGGTTCTGGCAGCACT-3′. (**B–D**) Knockdown of Rab11 isoforms. HeLa cells were transfected with control siRNA, Rab11a siRNA, Rab11b siRNA or siRNAs against both Rab11a and Rab11b as indicated, and processed for immunoblot analysis using an antibody against Rab11a (top panel), Rab11a+Rab11b (middle panel) or Rab5 (bottom panel; B), or double immunostaining for Rab11a+Rab11b and TfnR (C). Scale bar: 10 μm. (D) A hundred cells treated as in C were classified into those with Tfn-positive perinuclear vesicles (red), perinuclear tubules (blue) and structures around cellular tips (green).

Rab11a(S25N), caused accumulation of TfnR in the tip regions and delayed Tfn release as compared with cells expressing Rab11a(WT) (supplementary material Fig. S3A,B).

To further support that the exocytic event of internalized Tfn is suppressed in the Rab11-knockdown cells, we performed another experiment to chase internalized Tfn. Control HeLa cells or those treated with siRNAs for Rab11a and Rab11b were first incubated with Alexa-Fluor-488-conjugated Tfn at 37℃ for 5 min, and, after thoroughly washing out surface-bound fluorescent Tfn with acid, further incubated at 37℃ to chase internalized Tfn (supplementary material Fig. S4). Just after the 5 min pulse, fluorescent Tfn was found in punctate structures distributed throughout the cytoplasm in both the control and Rab11-knockdown cells (0 min chase), indicating that Tfn is normally internalized in the Rab11-knockdown cells. However, after 10 min chase at 37℃, internalized Tfn was considerably accumulated at the cell periphery in the Rab11-knockdown cells, whereas a significant fraction of internalized Tfn disappeared from the cells in the control cells. A similar trend was observed after 30 min chase. Thus, it is likely that the Rab11 depletion retards the exocytic process of internalized Tfn, but does not significantly affect the internalization.

Next, we asked whether the Tfn–TfnR complex that accumulates at the cell periphery is on or beneath the PM. For this purpose, cells treated with siRNAs for Rab11a+Rab11b were incubated with Alexa-Fluor-555–Tfn and immunostained with anti-TfnR antibody, which recognizes the exoplasmic/lumenal region of the TfnR protein, under either non-permeabilized or permeabilized conditions. If TfnR is on the cell surface, it will be detected under both conditions; whereas if it is in cytoplasmic vesicles it will be detected only under permeabilized conditions. In Rab11-knockdown cells, TfnR was detected in the tip regions only under permeabilized conditions (Fig. 3C), indicating accumulation of TfnR beneath the PM. This observation was confirmed by electron microscopy. We incubated Rab11-knockdown cells with horseradish peroxidase (HRP)-conjugated Tfn, and after allowing its endocytosis for 20 min, treated the cells with diaminobenzidine and H_2O_2. Under these conditions, clusters of Tfn-positive vesicles were found beneath the PM (Fig. 3D–F). Furthermore, Tfn-positive vesicles were often found along microtubule-like linear structures (Fig. 3E, yellow arrowheads). In the control cells, peripheral accumulation of Tfn-positive structures was less evident after 5 or 20 min endocytosis of HRP–Tfn (supplementary material Fig. S5, compare A and B), in agreement with the light microscopic data (Fig. 3A,B).

Microtubule-dependent transport of recycling carriers towards the cell periphery

Despite the drastic morphological change in TfnR-positive compartments by Rab11 depletion, the immunofluorescence and electron microscopic data (Fig. 3B–F) suggested that recycling carriers move toward the cell periphery and accumulate there. Both TfnR-positive vesicles in control cells and tubules in Rab11-knockdown cells were frequently found along microtubules (Fig. 3E, yellow arrowheads; Fig. 4A) suggesting that recycling carriers move along microtubules independently of Rab11. In addition, when TfnR–EGFP-expressing cells had been knocked down of Rab11 and recovery of fluorescence signals was followed by time-lapse imaging after photobleaching the peripheral TfnR–EGFP signals, tubular intermediates that appeared to extend from a proximal region gave rise to gradual recovery of peripheral signals (Fig. 4B; supplementary material Movie 3). To examine whether peripheral accumulation of TfnR depends on microtubules, we treated cells with nocodazole and, after removal of the drug, followed the change in localization of TfnR (Fig. 4C–E). When control cells were treated with nocodazole, neither Rab11 (Fig. 4C) nor TfnR (Fig. 4D) was found in the peripheral region (0 min panels). After nocodazole washout, however, both Rab11 and TfnR gradually accumulated around the cellular tips concomitant with microtubule reconstruction depicted by β-tubulin immunostaining (5–20 min panels). A similar time course of TfnR accumulation after nocodazole washout was

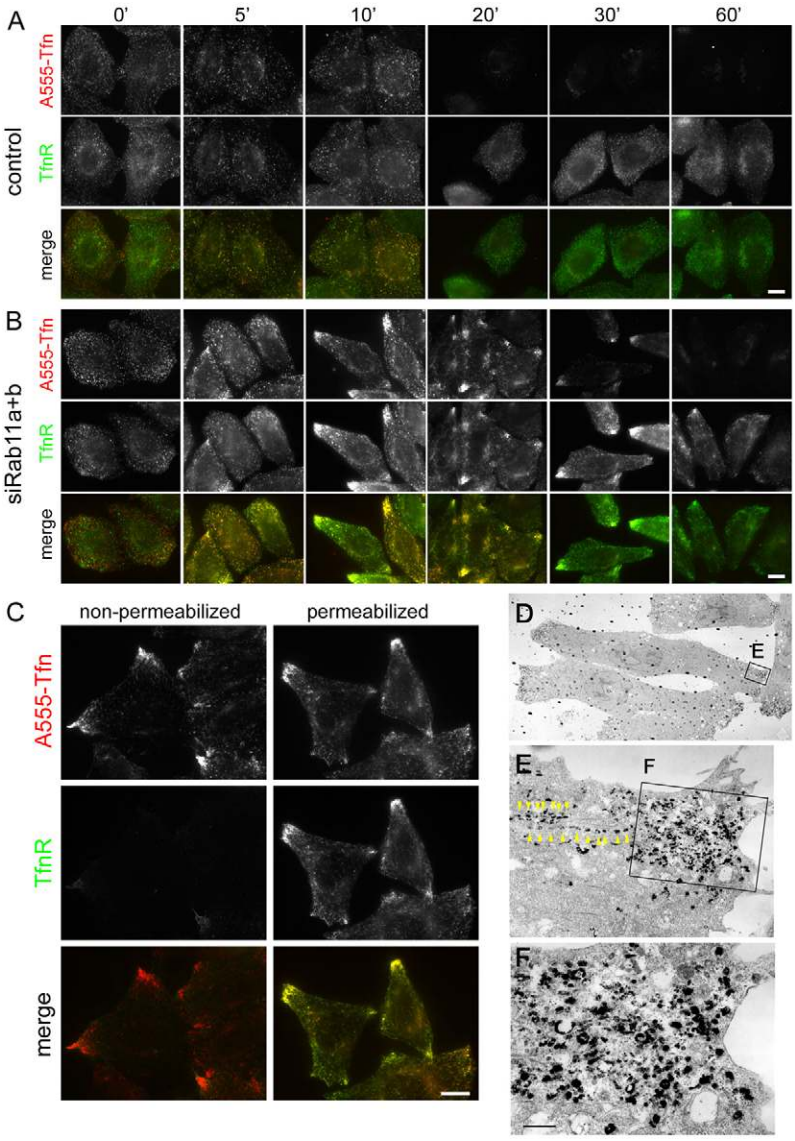

Fig. 3. Accumulation of recycled Tfn and TfnR beneath the PM in Rab11-depleted cells. (**A**,**B**) Accumulation of recycled Tfn and TfnR in Rab11-depleted cells. HeLa cells transfected with control siRNA (A) or siRNAs for Rab11a and Rab11b (B) were serum-starved for 3 h and incubated with Alexa-Fluor-555-conjugated Tfn at 4℃ for 50 min. After washing out excess fluorescent Tfn, the cells were then incubated in serum-containing medium at 37℃ for the indicated time periods and processed for immunostaining with anti-TfnR antibody. In Rab11-knockdown cells, there was substantial accumulation of Tfn and TfnR in the tip regions, in contrast to the control cells. (**C**) Accumulation of recycled Tfn and TfnR beneath the PM in Rab11-depleted cells. HeLa cells transfected with siRNAs for Rab11a and Rab11b were serum-starved for 3 h, incubated with Alexa-Fluor-555-conjugated Tfn at 4℃ for 50 min, washed, and incubated in a serum-containing medium at 37℃ for 20 min. The cells were fixed and either immediately (left column) or after permeabilization with 0.1% Triton X-100 (right column) incubated with monoclonal mouse anti-TfnR antibody, which recognizes the exoplasmic region of TfnR. In the Rab11-depleted cells, TfnR accumulated at the tips of pre-permeabilized cells only. (**D–F**) Electron microscopic analysis of accumulation of recycled Tfn beneath the PM. HeLa cells depleted of Rab11a and Rab11b were serum-starved for 3 h and incubated with HRP-conjugated Tfn at 4℃ for 50 min. After excess labeled Tfn was washed out, cells were incubated in a serum-containing medium at 37℃ for 20 min. The cells were then fixed, incubated with diaminobenzidine and H_2O_2 and processed for conventional electron microscopy. Note that clusters of vesicular structures positive for Tfn are present beneath the PM. Yellow arrowheads indicate Tfn-positive carriers lined up along microtubule-like structures. Scale bars: 10 μm (A–C); 0.5 μm (E).

observed in Rab11-depleted cells (Fig. 4E); a slight difference was that short tubular structures positive for TfnR were prominent during the recovery (10 min panel) in the Rab11-depleted cells (Fig. 4E) as compared with control cells (Fig. 4D). These observations, together with those in Fig. 1B and Fig. 3E and supplementary material Movie 1, support transport of Rab11- and TfnR-positive carriers along microtubules towards the cell periphery; however, the association with and transport along microtubules are independent of Rab11, albeit the drastic morphological change of the carriers in the absence of Rab11.

Rab11 and the exocyst are involved in exocytosis of recycling vesicles at the PM

How does Rab11 perturbation cause considerable accumulation of Tfn–TfnR-positive carrier intermediates beneath the PM? One possible explanation is that the final exocytic events are inhibited by loss of function of Rab11. To address this possibility, we applied total internal reflection fluorescence microscopy (TIRFM) to cells expressing TfnR–EGFP. In control cells, exocytic events of vesicles containing TfnR–EGFP were frequently observed, whereas lateral movement of these vesicles was infrequent (Fig. 5A; supplementary material Movie 4). In stark contrast, exocytic events were barely detectable in cells depleted of both Rab11 isoforms, and lateral movement of vesicular and tubular intermediates, probably along microtubules, was prominent (Fig. 5B; supplementary material Movie 5). Quantification of exocytic events revealed that exocytosis of TfnR–EGFP is ~20-fold less frequent in Rab11-knockdown cells than in control cells (Fig. 5F; 0.70±0.33 vs 13.8±3.1 exocytic events/cell/min). Thus, in Rab11-depleted cells, TfnR-containing vesicles appear to have no choice but to move laterally, due to their inability to find target membranes.

When cells expressing TfnR–EGFP and mCherry–Rab11a were subjected to dual-color TIRFM, significant populations of puncta observed are positive for both TfnR and Rab11a (Fig. 5C), indicating that TfnR and Rab11 are colocalized at the PM and/or just beneath the PM. This observation, together with the accumulation of TfnR-positive intermediates beneath the PM in the Rab11-knockdown cells, makes it possible that Rab11 participates in tethering and fusion of recycling vesicles with the PM. In the context of the exocytic event involving Rab11, we

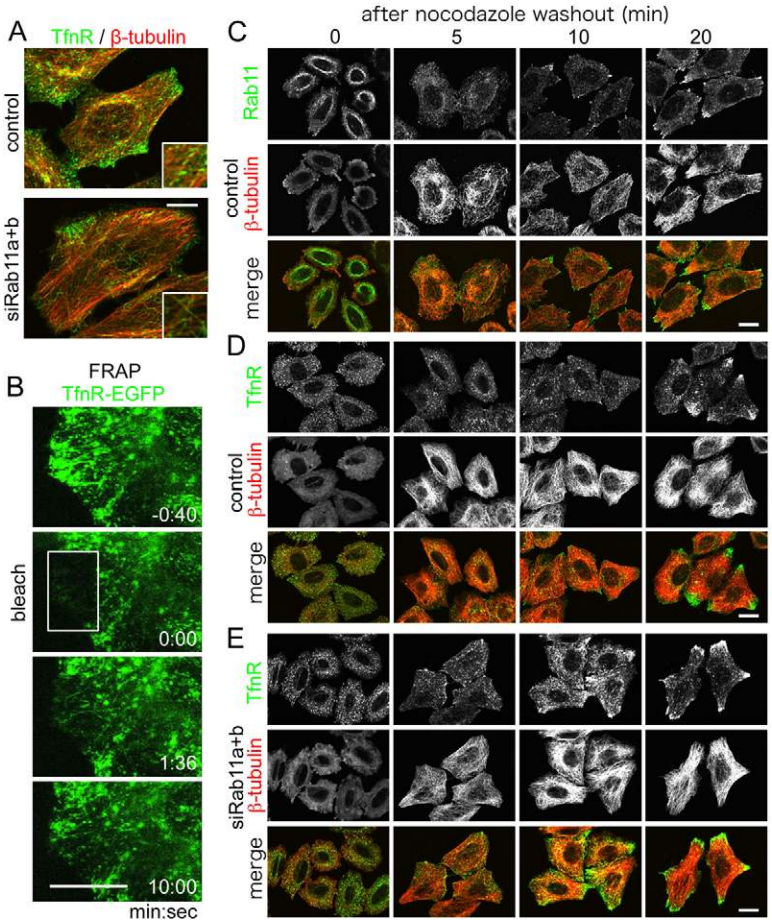

Fig. 4. Transport of TfnR-positive carrier intermediates to the cell periphery along microtubules. (**A**) Presence of TfnR-positive carrier intermediates along microtubules. HeLa cells were treated with control siRNA (upper panel) or siRNAs for Rab11a and Rab11b (lower panel) and doubly immunostained for TfnR and β-tubulin. (**B**) FRAP analysis of cells expressing TfnR–EGFP in which Rab11 had been knocked down. HeLa cells expressing TfnR–EGFP were transfected with siRNAs for Rab11a and Rab11b and subjected to FRAP analysis. At time=0, the boxed area was photobleached and signal recovery was followed by time-lapse recording. Representative frames from supplementary material Movie 3 are shown. Note that tubular structures extending from a proximal region, which may move along microtubules, are frequently observed. (**C–E**) Nocodazole treatment inhibits peripheral accumulation of TfnR. HeLa cells treated with control siRNA (C,D) or siRNAs for Rab11a and Rab11b (E) were incubated with 5 μg/ml nocodazole for 2 h, and, after washing out the drug, incubated in a normal medium for the indicated time periods. The cells were then doubly immunostained for β-tubulin and either Rab11 (C) or TfnR (D,E). Scale bars: 10 μm (A, C–E); 5 μm (B).

then focused on the exocyst tethering complex (He and Guo, 2009; Munson and Novick, 2006), because the exocyst has been implicated in Tfn recycling (Oztan et al., 2007; Prigent et al., 2003), and because Sec15, one subunit of the octameric protein complex, directly interacts with Rab11 (Wu et al., 2005; Zhang et al., 2004). In mammals, there are two Sec15 isoforms, Sec15A and Sec15B; we confirmed by RT-PCR that HeLa cells express both Sec15 isoforms (supplementary material Fig. S6A). Via immunoblotting using an available monoclonal anti-Sec15 antibody (Wang and Hsu, 2003), we detected three closely apposed bands in cell lysates (supplementary material Fig. S6B). Treatment of cells with a pool of siRNAs directed against Sec15A or Sec15B mRNA abolished the bottom or middle band, respectively; treating cells with both siRNA pools abolished the lower two bands (supplementary material Fig. S6B), indicating that the bottom and middle bands represent the Sec15A and Sec15B proteins, respectively; the top band may be non-specific. When HeLa cells were depleted of either Sec15A or Sec15B alone, Tfn–TfnR recycling was marginally affected (supplementary material Fig. S6C, columns 2 and 3). In contrast, simultaneous knockdown of both Sec15 isoforms considerably delayed Tfn–TfnR recycling and accumulation of recycled Tfn and TfnR in the tip regions (Fig. 6B; supplementary material Fig. S6C, right column). When examined by TIRFM, TfnR–EGFP-positive carriers barely fused with the PM in cells treated with both Sec15A and Sec15B siRNAs (Fig. 5D; supplementary material Movie 6). Quantification of the exocytic events revealed that the exocytic frequency of TfnR–EGFP-positive carriers in Sec15-knockdown cells is approximately one-seventh of that in control cells (Fig. 5F; 1.87±0.32 vs 13.8±3.1 exocytic events/cell/min).

These observations suggest that the exocyst participates in the final exocytic events, i.e. tethering and fusion of carrier vesicles, downstream of Rab11. Attempting to exclude potential off-target effects of the Sec15 siRNAs, we examined whether exogenously expressed Sec15 could rescue the Sec15-knockdown phenotypes. However, exogenously expressed Sec15 formed aggregates in the cytoplasm and appeared to disturb Tfn recycling (data not shown), probably because the excess Sec15 protein could not form a functional exocyst complex together with other endogenous subunits. To circumvent this problem, and investigate whether the exocyst complex participates en bloc in the exocytic event, we turned to another subunit, Exo70, chosen because an available anti-Exo70 antibody (Vega and Hsu, 2001) works well in both immunoblotting and immunofluorescence. Exo70 was significantly colocalized with Rab11 in the peripheral region (Fig. 7A, left column). Moreover, we found that Exo70 was also colocalized with Rab11 in the perinuclear region (Fig. 7A, right column). This was rather unexpected, because several studies reported that the exocyst components, including Exo70, associate mainly with the PM through interacting with PtdIns(4,5)P_2 in yeast and mammalian cells (He and Guo, 2009; He et al., 2007; Liu et al., 2007), although localization of the exocyst to Tfn-positive endosomes was also reported (Oztan et al., 2007). We therefore examined whether Rab11 depletion influences the Exo70 localization and found that depletion of Rab11a and Rab11b redistributed Exo70 from the perinuclear region to the cytoplasm

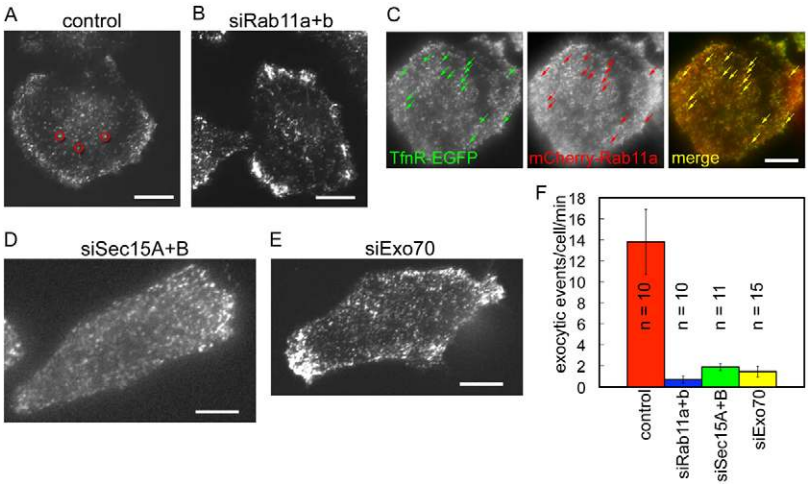

Fig. 5. Knockdown of Rab11 or exocyst subunit inhibits exocytic events of TfnR–EGFP-containing vesicles. (**A**,**B**,**D–F**) HeLa cells stably expressing TfnR–EGFP were transfected with control siRNA (A), or siRNAs against Rab11a and Rab11b (B), Sec15A and Sec15B (D) or Exo70 (E), and subjected to TIRFM. Representative frames from the corresponding supplementary material Movies 4–7 are shown. (F) Exocytic events detected per minute in single cells were counted in each case. The values are means ± s.d. of 10 (A), 10 (B), 11 (C) and 15 (D) cells. Scale bars: 10 µm. (**C**) HeLa cells stably expressing TfnR–EGFP were transfected with an expression vector for N-terminally mCherry-tagged Rab11a, fixed with 3% paraformaldehyde and subjected to dual-color TIRFM. Arrows indicate representative puncta with both the TfnR and Rab11a signals.

(Fig. 7C, middle column, cells indicated by asterisks), although apparently did not alter the cellular level of the Exo70 protein (Fig. 7B); this observation indicates that Rab11 is involved in membrane recruitment of the exocyst at perinuclear REs. On the other hand, depletion of Exo70 changed Rab11 localization; specifically, Rab11 was significantly accumulated in the tip regions (Fig. 7C, right column). Furthermore, as with Rab11 depletion, Exo70 depletion resulted in accumulation of recycled Tfn and TfnR at the cell periphery (Fig. 6C) and a decrease in the exocytic frequency of TfnR-positive vesicles (Fig. 5E,F; supplementary material Movie 7). These observations together indicate that Rab11 and probably the exocyst are transported from

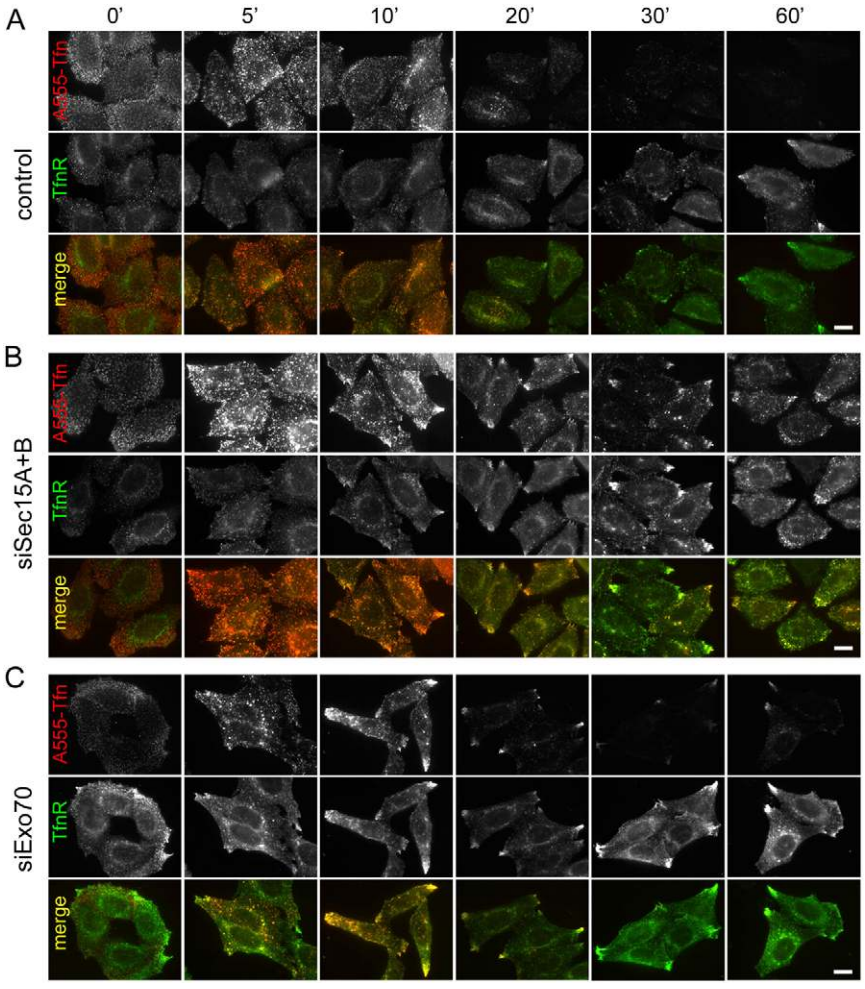

Fig. 6. Accumulation of recycled Tfn and TfnR at the cell periphery in cells depleted of exocyst subunits. HeLa cells transfected with (**A**) control siRNAs or siRNAs against (**B**) Sec15A and Sec15B or (**C**) Exo70 were processed as described for Fig. 3A,B. Scale bars: 10 µm.

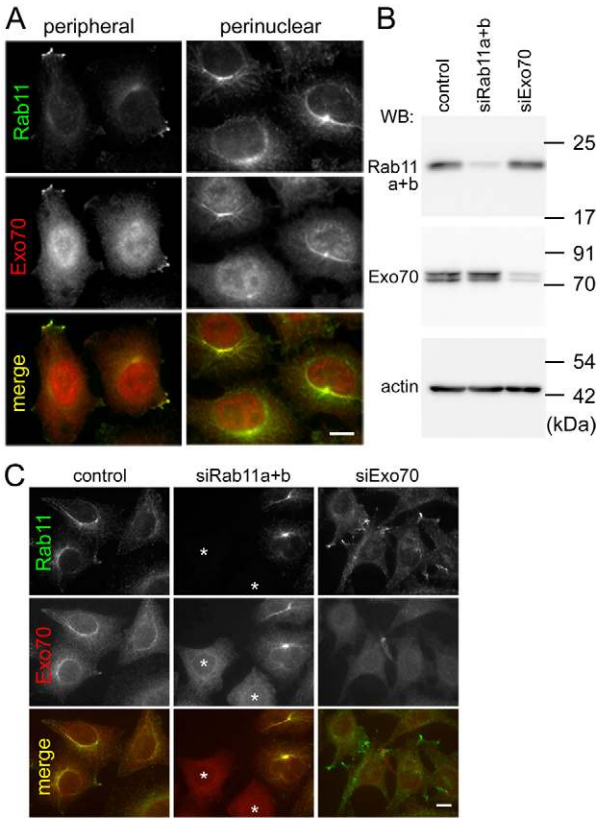

Fig. 7. Localization and knockdown of Exo70 in HeLa cells. (**A**) Comparison of localization of endogenous Rab11 and Exo70. HeLa cells were doubly immunostained for Rab11 and Exo70. Microscopic images were acquired by focusing on the plane where the peripheral (left panels) or perinuclear (right panels) staining was evident. (**B**,**C**) HeLa cells were transfected with control siRNA, siRNAs against both Rab11a and Rab11b or Exo70 siRNA as indicated, and processed for immunoblot analysis with antibodies against Rab11a+Rab11b, Exo70 or β-actin (B), or double immunostaining for Rab11a+Rab11b and Exo70 (C). Cells efficiently depleted of Rab11 are indicated by asterisks. Scale bars: 10 μm.

perinuclear REs through associating with recycling vesicles and participate in tethering and fusion of these vesicles with the PM.

Discussion

We have shown here that Rab11 is involved in regulation of the final exocytic event of recycling carriers at the PM, although it is well known to associate with perinuclear REs. Rab11 perturbation (siRNA-mediated depletion of endogenous Rab11 or expression of a dominant-negative mutant) results in accumulation of vesicles containing endocytosed Tfn and TfnR at the cell periphery, particularly in cellular tip regions. The recycling carriers appear to be transported along microtubules from the perinuclear to peripheral regions. The TIRFM data unequivocally demonstrate that Rab11 depletion inhibits exocytic events of recycling vesicles. Rab11 depletion also results in redistribution of Exo70 to the cytoplasm, suggesting that membrane association of the exocyst is, at least in part, under the regulation of Rab11; the exocyst may be recruited onto membranes at perinuclear REs and transported to the cell periphery together with Rab11. As predicted from the interaction of Rab11 with the exocyst, knockdown of Sec15 or Exo70 leads to essentially the same phenotypes (accumulation of recycling carriers beneath the PM) as those exhibited by Rab11-knockdown cells, as well as peripheral accumulation of Rab11. The most plausible explanation for these observations is that inhibition of tethering of Rab11-positive vesicles results in vesicle accumulation beneath the PM; this is consistent with previous studies showing that Rab11 accumulated in the apical portion of epithelial cells in *Drosophila* exocyst mutants (Langevin et al., 2005), and that Rab11 diffused from vesicle-like dots into the PM, concurrent with exocytosis of Fc receptor–positive vesicles (Ward et al., 2005). Thus, the role of Rab11 at the PM is consistent with the general view of the roles of Rab GTPases in membrane tethering and fusion (Zerial and McBride, 2001).

What is the role of Rab11 at perinuclear REs? The TfnR-positive tubules observed in Rab11-perturbed cells may result from failure of fission of vesicles budding from REs. Thus, in addition to its role in tethering of recycling vesicles with the PM, Rab11 may also participate in vesicle formation from REs. Despite their roles in membrane tethering and fusion, several Rab GTPases have been implicated in controlling vesicle budding (Stenmark, 2009). In particular, the yeast counterparts of Rab11, Ypt31 and Ypt32, are required for vesicle budding from the *trans*-Golgi network (Jedd et al., 1997). In this context, it is noteworthy that knockdown of Arf family small GTPases, in particular, simultaneous knockdown of class I Arfs (Arf1 and Arf3), causes tubulation of Tfn-positive compartments and delay of Tfn recycling (Volpicelli-Daley et al., 2005); vesicle budding is well known to be regulated by Arfs (D'Souza-Schorey and Chavrier, 2006). It is therefore tempting to speculate that Arfs and Rab11 function along the same sequence of a recycling event from REs. Despite the dramatic tubulation of TfnR-positive REs in Rab11-depleted cells, recycling carriers containing Tfn and TfnR were still delivered to the cell periphery in a microtubule-dependent manner (Fig. 4E). Thus, although Rab11 is required for tethering/fusion of recycling carriers with the PM as shown by the TIRFM analysis (Fig. 5B), it is dispensable for the association of recycling carriers with microtubules.

Taken together, we propose the following model for Rab11 functions in Tfn–TfnR recycling. (1) Rab11 participates in the exit of recycling vesicles from perinuclear REs. (2) Recycling vesicles are transported along microtubules towards the cell periphery, although Rab11 per se is not required for microtubule association of recycling intermediates. (3) Finally, Rab11 regulates tethering of recycling vesicles with the PM in concert with the exocyst. In the future, it will be important to identify the SNARE proteins that are involved in the final fusion of recycling vesicles with the PM.

Materials and Methods

Antibodies and reagents

Monoclonal mouse anti-Exo70 and anti-Sec15 antibodies were kind gifts from Shu-Chan Hsu (Rutgers University) and Wei Guo (University of Pennsylvania), respectively (Vega and Hsu, 2001; Wang and Hsu, 2003). Polyclonal rabbit anti-Rab11 antibody, which reacts with Rab11a, and monoclonal mouse anti-TfnR antibody (H68.4), which recognizes a cytoplasmic epitope, were purchased from Zymed (South San Francisco, CA). Monoclonal mouse anti-TfnR/CD71 antibody, which recognizes an exoplasmic/lumenal epitope, was from Sigma-Aldrich (St Louis, MO). Monoclonal mouse anti-Rab11 antibody, which reacts with both Rab11a and Rab11b, and monoclonal mouse antibodies to Rab5, EEA1, Lamp-1 and GM130 were from BD Biosciences (Franklin Lakes, NJ). Monoclonal mouse antibodies to β-tubulin and β-actin were from Millipore (Billerica, MA). Monoclonal rat anti-HA antibody was from Roche Applied Science (Indianapolis, IN). Alexa-Fluor- and HRP-conjugated secondary antibodies were from Molecular Probes (Carlsbad, CA) and Jackson ImmunoResearch Laboratories (West Grove, PA), respectively. Alexa-Fluor- and HRP-conjugated Tfn were

from Molecular Probes and Jackson ImmunoResearch Laboratories, respectively. Nocodazole was from Sigma-Aldrich.

Plasmids

An expression vector encoding human DMT1-II tagged with EGFP (Tabuchi et al., 2002) was a kind gift from Mitsuaki Tabuchi (Kagawa University, Japan). N-terminally HA- and EGFP-tagged Rab11a expression vectors were constructed by subcloning a cDNA fragment containing the coding sequence of human Rab11a into pcDNA3-HAN (Shin et al., 1997) and pEGFP-C1 (Clontech, Mountain View, CA), respectively. Construction of an expression vector for N-terminally mCherry-tagged Rab11a was described previously (Takahashi et al., 2011). The S25N mutation was introduced into the Rab11a cDNA using a Quik Change Site-Directed Mutagenesis kit (Agilent Technologies, Santa Clara, CA).

Plasmids for production of replication-defective, self-inactivating lentiviral vectors, pRRLsinPPT, and packaging plasmids (pRSV-REV, pMD2.g and pMDLg/pRRE) (Thomas et al., 2009) were kindly provided by Peter McPherson (McGill University, Canada). A destination cassette from pcDNA3.2/V5-DEST (Invitrogen, Carlsbad, CA) was inserted into pRRLsinPPT in order to convert it to a Gateway system destination vector; the resultant plasmid was named pRRLsinPPT-DEST. A plasmid vector for lentiviral production of human TfnR tagged with MEF (Myc-TEV-Flag; a kind gift from Toshiaki Isobe, Tokyo Metropolitan University) (Ichimura et al., 2005) and EGFP was constructed by subcloning a DNA fragment encoding MEF-TfnR-EGFP into pENTR3C-dual (Invitrogen); the resulting gene was then transferred into pRRLsinPPT-DEST using the Clonase LR recombination reaction (Invitrogen). The resultant plasmid, pRRLsinPPT-MEF-TfnR-EGFP, was used for lentiviral vector production.

DNA transfection and RNA interference experiment

Plasmid DNAs were transfected into HeLa cells using the FuGENE6 transfection reagent according to the manufacturer's instructions (Roche Applied Science). The Rab11a and Rab11b isoforms (Takahashi et al., 2011), and Exo70 (Zuo et al., 2006) were knocked down using double-stranded siRNAs purchased from Dharmacon, as described previously. Briefly, HeLa cells were transfected with the siRNAs using Lipofectamine 2000 (Invitrogen) and incubated for 24 h. The cells were then transferred to a new culture dish, incubated for an additional 48 h, and processed for immunofluorescence or immunoblot analysis. For knockdown of Sec15A or Sec15B, pools of siRNAs directed against the 3′-untranslated region of human Sec15A and Sec15B mRNAs (nucleotide residues 2424–3247 and 2454–2990, respectively, when the A residue of the initiation Met codon is assigned as residue 1), were prepared using the BLOCK-iT RNAi TOPO Transcription Kit and BLOCK-iT Dicer RNAi Kit (Invitrogen). HeLa cells were treated with the siRNA pools and processed for immunofluorescence or immunoblot analysis as described above for Rab11 and Exo70 knockdowns.

Lentiviral vector production and establishment of cell lines stably expressing MEF-TfnR–EGFP

pRRLsinPPT-MEF-TfnR-EGFP was transfected into HEK293FT cells (Invitrogen) using Polyethylenimine Max (Polysciences, Warrington, PA) along with the packaging plasmids (pRSV-REV, pMD2.g and pMDL/pRRE). Culture medium was replaced 8 h after transfection. Culture media containing the lentiviral vector were collected at 24, 36 and 48 h after transfection, filtrated through a 0.45-μm filter (Millipore) and centrifuged at 32,000 ***g*** at 4℃ for 4 h in an R15A rotor and Himac CR22G centrifuge (Hitachi Koki, Tokyo, Japan). The precipitated viral vector was resuspended in minimal essential medium.

HeLa cell lines stably expressing MEF-TfnR–EGFP were established by transduction with the lentiviral vector and isolated using cloning cylinders. One of the selected HeLa(MEF-TfnR–EGFP) clones, clone 6, was used in the following experiments.

Immunofluorescence microscopy, time-lapse imaging, TIRFM and fluorescence recovery after photobleaching analysis

Immunofluorescence analysis of cells was performed as described previously (Takahashi et al., 2011). Briefly, cells were fixed with 3% paraformaldehyde at room temperature for 10 min, washed three times with phosphate-buffered saline (PBS), quenched with 50 mM NH_4Cl for 20 min, washed three times with PBS, permeabilized with 0.1% Triton X-100 in PBS for 5 min, and washed three times with PBS. For detection of Rab11, cells were fixed with 10% trichloroacetic acid on ice for 15 min. The fixed/permeabilized cells were then subjected to staining with antibodies diluted with Can Get Signal immunostain (TOYOBO, Osaka, Japan), and observed using an Axiovert 200M microscope (Carl Zeiss, Göttingen, Germany) or an A1R-MP confocal laser-scanning microscope (Nikon, Tokyo, Japan).

For time-lapse recording, HeLa cells were plated on a collagen-coated glass-bottom culture dish (Mat Tek Corp.). Twenty-four hours after plating, an expression plasmid encoding EGFP-tagged Rab11a was transfected into the cells using a FuGENE6 reagent. After 48 h incubation, cells were mounted on a Stage Top Incubator (Tokai Hit, Fujinomiya, Japan). Cells were imaged at 37℃ on an inverted microscope (Axiovert 200M) using a 63× oil immersion lens and a charge-coupled device camera (C9100-02; Hamamatsu Photonics, Hamamatsu, Japan). Time-lapse images were taken sequentially every 30 sec and analyzed using the MetaMorph imaging software (Molecular Devices, Sunnyvale, CA). Movies correspond to three frames per second.

For TIRFM, HeLa cells stably expressing TfnR–EGFP were culture on a 35-mm culture dish for 24 h, transfected with siRNAs, and further incubated for 24 h. The transfected cells were then transferred to a collagen-coated glass-bottom culture dish. After 48 h incubation, the cells were incubated in HEPES-buffered modified Eagle's medium, placed on a microscope stage pre-warmed to 37℃, and observed using NIS-Elements imaging software on a TIRFM ECLIPSE Ti (Nikon).

For time-lapse analysis after photobleaching (FRAP), cells expressing EGFP–Rab11a or those expressing TfnR–EGFP treated with siRNAs for Rab11a and Rab11b were incubated in HEPES-buffered modified Eagle's medium and placed on a microscope stage that was preincubated at 37℃. The cells were observed and bleached using FV1000D on an inverted microscope IX81 (Olympus, Tokyo, Japan) or the A1R-MP confocal microscope. To visualize FRAP of TfnR–EGFP, images were acquired sequentially every 2 seconds. Movies were recorded at 3 or 10 frames/sec.

Electron microscopy

Cells treated with control siRNA or siRNAs for Rab11a and Rab11b were incubated with HRP-conjugated Tfn (50 μg/ml) for 50 min at 4℃, washed, and then incubated for 5 or 20 min at 37℃. They were fixed with 3% paraformaldehyde in 0.1 M phosphate buffer (pH 7.2), and incubated first with diaminobenzidine (500 ng/ml) in 0.1 M Tris-HCl (pH 7.6) for 5 h, then with the same solution containing 0.005% H_2O_2 for 15 min at room temperature. The cells were further fixed with 2% glutaraldehyde–2% paraformaldehyde in 0.1 M phosphate buffer (pH 7.2) and embedded in Epon812 for conventional electron microscopy as described previously (Waguri et al., 1999).

Acknowledgements

We thank Shu-Chan Hsu, Wei Guo, Mitsuaki Tabuchi, Peter McPherson and Toshiaki Isobe for providing materials, and Katsuyuki Kanno and Akane Yamada for electron microscopy.

Funding

This work was supported by grants from the Ministry of Education, Culture, Sports, Science and Technology of Japan [grant number 22390013 to K.N.]; and the Targeted Proteins Research Program [grant number 07069031 to K.N.].

Supplementary material available online at
http://jcs.biologists.org/lookup/suppl/doi:10.1242/jcs.102913/-/DC1

References

D'Souza-Schorey, C. and Chavrier, P. (2006). ARF proteins: roles in membrane traffic and beyond. *Nat. Rev. Mol. Cell Biol.* **7**, 347-358.

Grant, B. D. and Donaldson, J. G. (2009). Pathways and mechanisms of endocytic recycling. *Nat. Rev. Mol. Cell Biol.* **10**, 597-608.

Guichard, A., McGillivray, S. M., Cruz-Moreno, B., van Sorge, N. M., Nizet, V. and Bier, E. (2010). Anthrax toxins cooperatively inhibit endocytic recycling by the Rab11/Sec15 exocyst. *Nature* **467**, 854-858.

He, B. and Guo, W. (2009). The exocyst complex in polarized exocytosis. *Curr. Opin. Cell Biol.* **21**, 537-542.

He, B., Xi, F., Zhang, X., Zhang, J. and Guo, W. (2007). Exo70 interacts with phospholipids and mediates the targeting of the exocyst to the plasma membrane. *EMBO J.* **26**, 4053-4065.

Hölttä-Vuori, M., Tanhuanpää, K., Möbius, W., Somerharju, P. and Ikonen, E. (2002). Modulation of cellular cholesterol transport and homeostasis by Rab11. *Mol. Biol. Cell* **13**, 3107-3122.

Ichimura, T., Yamamura, H., Sasamoto, K., Tominaga, Y., Taoka, M., Kakiuchi, K., Shinkawa, T., Takahashi, N., Shimada, S. and Isobe, T. (2005). 14-3-3 proteins modulate the expression of epithelial Na^+ channels by phosphorylation-dependent interaction with Nedd4-2 ubiquitin ligase. *J. Biol. Chem.* **280**, 13187-13194.

Jedd, G., Mulholland, J. and Segev, N. (1997). Two new Ypt GTPases are required for exit from the yeast *trans*-Golgi compartment. *J. Cell Biol.* **137**, 563-580.

Junutula, J. R., Schonteich, E., Wilson, G. M., Peden, A. A., Scheller, R. H. and Prekeris, R. (2004). Molecular characterization of Rab11 interactions with members of the family of Rab11-interacting proteins. *J. Biol. Chem.* **279**, 33430-33437.

Lam-Yuk-Tseung, S. and Gros, P. (2006). Distinct targeting and recycling properties of two isoforms of the iron transporter DMT1 (NRAMP2, Slc11A2). *Biochemistry* **45**, 2294-2301.

Langevin, J., Morgan, M. J., Sibarita, J. B., Aresta, S., Murthy, M., Schwarz, T., Camonis, J. and Bellaïche, Y. (2005). *Drosophila* exocyst components Sec5, Sec6, and Sec15 regulate DE-Cadherin trafficking from recycling endosomes to the plasma membrane. *Dev. Cell* **9**, 365-376.

Liu, J., Zuo, X., Yue, P. and Guo, W. (2007). Phosphatidylinositol 4,5-bisphosphate mediates the targeting of the exocyst to the plasma membrane for exocytosis in mammalian cells. *Mol. Biol. Cell* **18**, 4483-4492.
Maxfield, F. R. and McGraw, T. E. (2004). Endocytic recycling. *Nat. Rev. Mol. Cell Biol.* **5**, 121-132.
Mukherjee, S., Ghosh, R. N. and Maxfield, F. R. (1997). Endocytosis. *Physiol. Rev.* **77**, 759-803.
Munson, M. and Novick, P. (2006). The exocyst defrocked, a framework of rods revealed. *Nat. Struct. Mol. Biol.* **13**, 577-581.
Oztan, A., Silvis, M., Weisz, O. A., Bradbury, N. A., Hsu, S.-C., Goldenring, J. R., Yeaman, C. and Apodaca, G. (2007). Exocyst requirement for endocytic traffic directed toward the apical and basolateral poles of polarized MDCK cells. *Mol. Biol. Cell* **18**, 3978-3992.
Prigent, M., Dubois, T., Raposo, G., Derrien, V., Tenza, D., Rossé, C., Camonis, J. and Chavrier, P. (2003). ARF6 controls post-endocytic recycling through its downstream exocyst complex effector. *J. Cell Biol.* **163**, 1111-1121.
Ren, M., Xu, G., Zeng, J., De Lemos-Chiarandini, C., Adesnik, M. and Sabatini, D. D. (1998). Hydrolysis of GTP on rab11 is required for the direct delivery of transferrin from the pericentriolar recycling compartment to the cell surface but not from sorting endosomes. *Proc. Natl. Acad. Sci. USA* **95**, 6187-6192.
Schwartz, S. L., Cao, C., Pylypenko, O., Rak, A. and Wandinger-Ness, A. (2007). Rab GTPases at a glance. *J. Cell Sci.* **120**, 3905-3910.
Shin, H.-W., Shinotsuka, C., Torii, S., Murakami, K. and Nakayama, K. (1997). Identification and subcellular localization of a novel mammalian dynamin-related protein homologous to yeast Vps1p and Dnm1p. *J. Biochem.* **122**, 525-530.
Stenmark, H. (2009). Rab GTPases as coordinators of vesicle traffic. *Nat. Rev. Mol. Cell Biol.* **10**, 513-525.
Tabuchi, M., Tanaka, N., Nishida-Kitayama, J., Ohno, H. and Kishi, F. (2002). Alternative splicing regulates the subcellular localization of divalent metal transporter 1 isoforms. *Mol. Biol. Cell* **13**, 4371-4387.
Takahashi, S., Takei, T., Koga, H., Takatsu, H., Shin, H.-W. and Nakayama, K. (2011). Distinct roles of Rab11 and Arf6 in the regulation of Rab11-FIP3/arfophilin-1 localization in mitotic cells. *Genes Cells* **16**, 938-950.
Thomas, S., Ritter, B., Verbich, D., Sanson, C., Bourbonnière, L., McKinney, R. A. and McPherson, P. S. (2009). Intersectin regulates dendritic spine development and somatodendritic endocytosis but not synaptic vesicle recycling in hippocampal neurons. *J. Biol. Chem.* **284**, 12410-12419.
Ullrich, O., Reinsch, S., Urbé, S., Zerial, M. and Parton, R. G. (1996). Rab11 regulates recycling through the pericentriolar recycling endosome. *J. Cell Biol.* **135**, 913-924.
van Ijzendoorn, S. C. D. (2006). Recycling endosomes. *J. Cell Sci.* **119**, 1679-1681.
Vega, I. E. and Hsu, S.-C. (2001). The exocyst complex associates with microtubules to mediate vesicle targeting and neurite outgrowth. *J. Neurosci.* **21**, 3839-3848.
Volpicelli-Daley, L. A., Li, Y., Zhang, C.-J. and Kahn, R. A. (2005). Isoform-selective effects of the depletion of ADP-ribosylation factors 1-5 on membrane traffic. *Mol. Biol. Cell* **16**, 4495-4508.
Waguri, S., Kohmura, M., Gotow, T., Watanabe, T., Ohsawa, Y., Kominami, E. and Uchiyama, Y. (1999). The induction of autophagic vacuoles and the unique endocytic compartments, C-shaped multivesicular bodies, in GH_4C_1 cells after treatment with 17β-estradiol, insulin and EGF. *Arch. Histol. Cytol.* **62**, 423-434.
Wang, S. and Hsu, S.-C. (2003). Immunological characterization of exocyst complex subunits in cell differentiation. *Hybrid. Hybridomics* **22**, 159-164.
Ward, E. S., Martinez, C., Vaccaro, C., Zhou, J., Tang, Q. and Ober, R. J. (2005). From sorting endosomes to exocytosis: association of Rab4 and Rab11 GTPases with the Fc receptor, FcRn, during recycling. *Mol. Biol. Cell* **16**, 2028-2038.
Wilcke, M., Johannes, L., Galli, T., Mayau, V., Goud, B. and Salamero, J. (2000). Rab11 regulates the compartmentalization of early endosomes required for efficient transport from early endosomes to the trans-golgi network. *J. Cell Biol.* **151**, 1207-1220.
Wu, S., Mehta, S. Q., Pichaud, F., Bellen, H. J. and Quiocho, F. A. (2005). Sec15 interacts with Rab11 via a novel domain and affects Rab11 localization in vivo. *Nat. Struct. Mol. Biol.* **12**, 879-885.
Zerial, M. and McBride, H. (2001). Rab proteins as membrane organizers. *Nat. Rev. Mol. Cell Biol.* **2**, 107-117.
Zhang, X.-M., Ellis, S., Sriratana, A., Mitchell, C. A. and Rowe, T. (2004). Sec15 is an effector for the Rab11 GTPase in mammalian cells. *J. Biol. Chem.* **279**, 43027-43034.
Zuo, X., Zhang, J., Zhang, Y., Hsu, S. C., Zhou, D. and Guo, W. (2006). Exo70 interacts with the Arp2/3 complex and regulates cell migration. *Nat. Cell Biol.* **8**, 1383-1388.